Electronic Supplementary Material (ESI) for Soft Matter.

Supplementary Information

Nature inspired solid-liquid phase amphibious adhesive

Alin Cristian Chipara,[1] Gustavo Brunetto,[1,2] Sehmus Ozden,[1] Henrik Haspel,[1,3] Partha Kumbhakar,[7] Ken Hackenberg,[1] Mohamad Kabbani,[1] Balázs Buchhocz,[3] Ákos Kukovecz,[3,5] Zoltán Kónya,[3,6] Robert Vajtai,[1] Mircea Chipara,[4] Douglas S. Galvao,[2] Chandra Shaker Tiwary,[1,7*] and Pulickel M. Ajayan[1*]

[1]Department of Materials Science and Nano Engineering, Rice University, Houston, TX, 77005, USA

[2]Department of Applied Physics and Center for Computational Engineering & Sciences , State University of Campinas, Campinas, SP, 13083-959, Brazil

[3]Department of Applied and Environmental Chemistry, University of Szeged, RerrichBélatér 1, Szeged H-6720, Hungary

[4]Department of Physics and Geology, University of Texas-Pan American, Edinburg, TX 78539, USA

[5]MTA-SZTE "Lendület" Porous Nanocomposites Research Group, RerrichBélatér 1, Szeged H-6720, Hungary

[6]MTA-SZTE Reaction Kinetics and Surface Chemistry Research Group, RerrichBélatér 1, Szeged H-6720, Hungary

[7]Metallurgical and Materials Engineering, Indian Institute of Technology Kharagpur, Kharagpur-721302, India.

Corresponding Authors: E-mail: ajayan@rice.edu (P. M. Ajayan), cst.iisc@gmail.com (C. S. Tiwary)

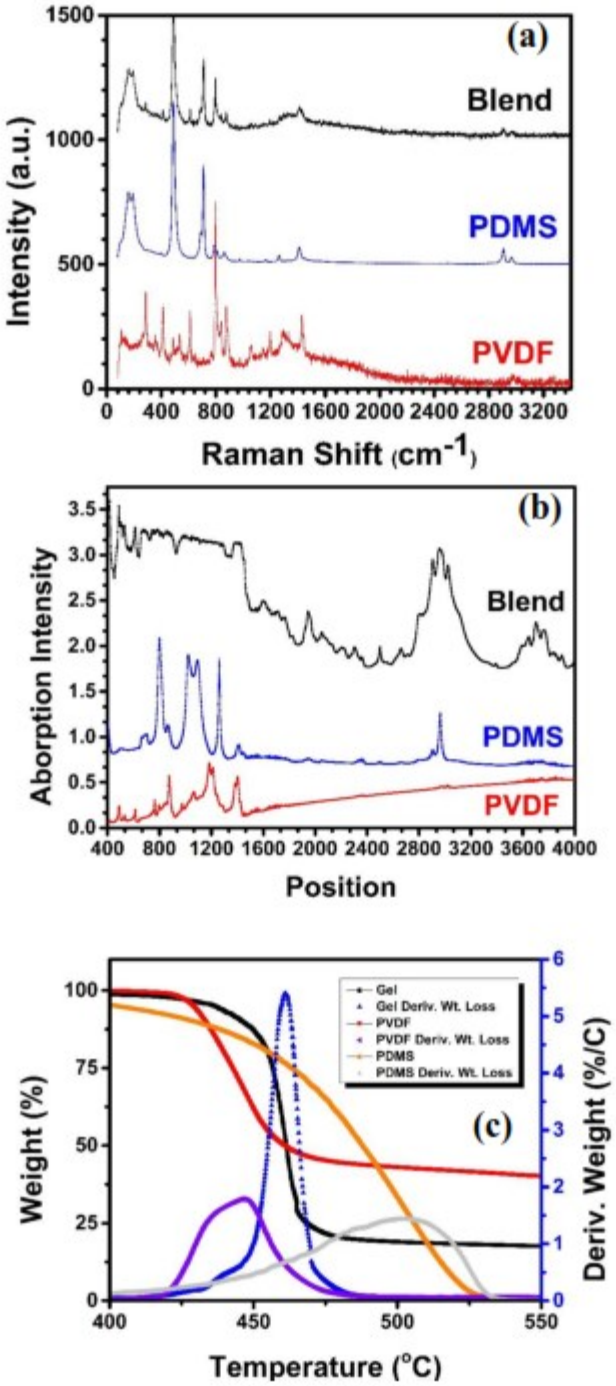

Fig. S1. Spectroscopic and Thermal Measurements*:* a) Raman of PVDF (seen in red), PDMS (seen in blue), and the blend (seen in black). The Raman shows that no new bonds are formed within the blend and that it is a convolution of the two homopolymers. b) FTIR taken at room

temperature in ambient conditions shows some change in the spectra with the loss of some peaks and some gaining much more intensity (O-H bonds show a noticeable increase). c) TGA results show PVDF in red, PDMS in orange and the blend in black. The blend shows increased thermal stability in relation to the homopolymers. The peaks represent the derivative weight loss of the material. PVDF is shown in purple and PDMS in grey and the blend is in blue. A bimodal peak would be expected in a polymer blend; however, only one peak can be seen.

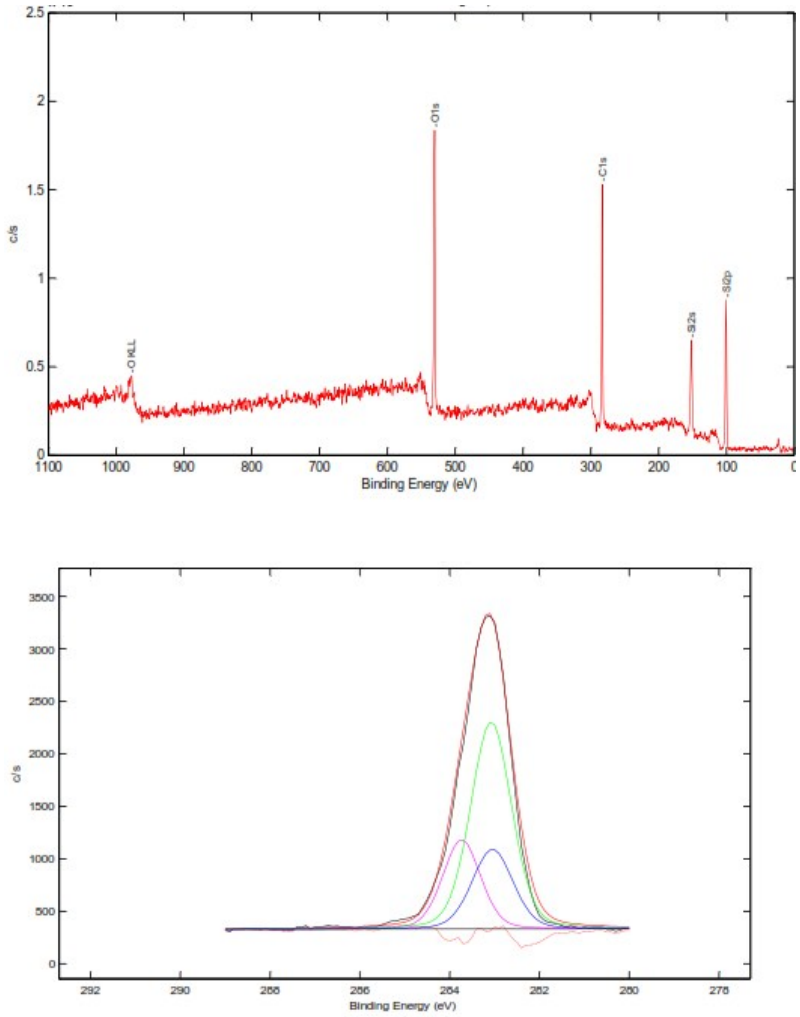

Fig. S2. XPS Data: The figure shows the XPS data for the blend. XPS reveals the presence of Si which means that the F atoms should be fully coated by the PDMS.

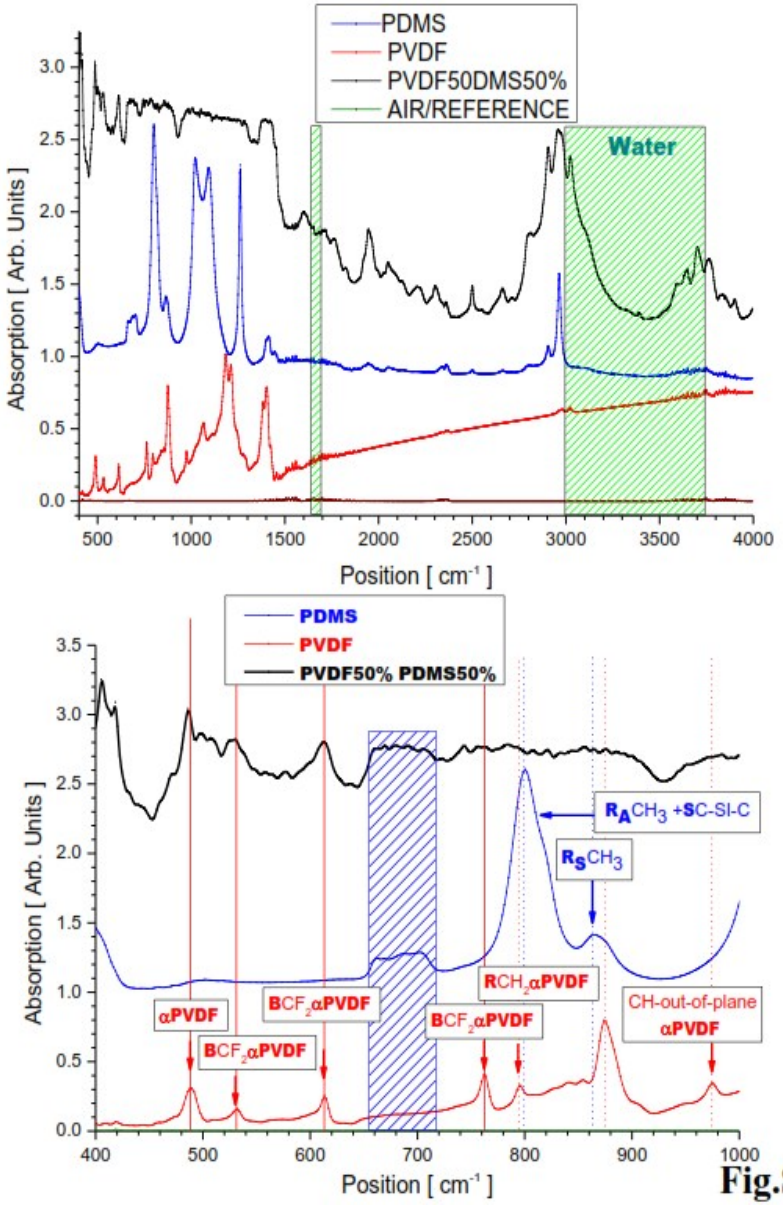
PDMS
PVDF
PVDF50DMS50%
AIR/REFERENCE
Water
Absorption [Arb. Units]
Position [cm-1]
PDMS
PVDF
PVDF50% PDMS50%
RACH3 +SC-SI-C
RSCH3
RCH2αPVDF
CH-out-of-plane
αPVDF
αPVDF
BCF2αPVDF
BCF2αPVDF
BCF2αPVDF
Absorption [Arb. Units]
Position [cm-1]

Fig.S3

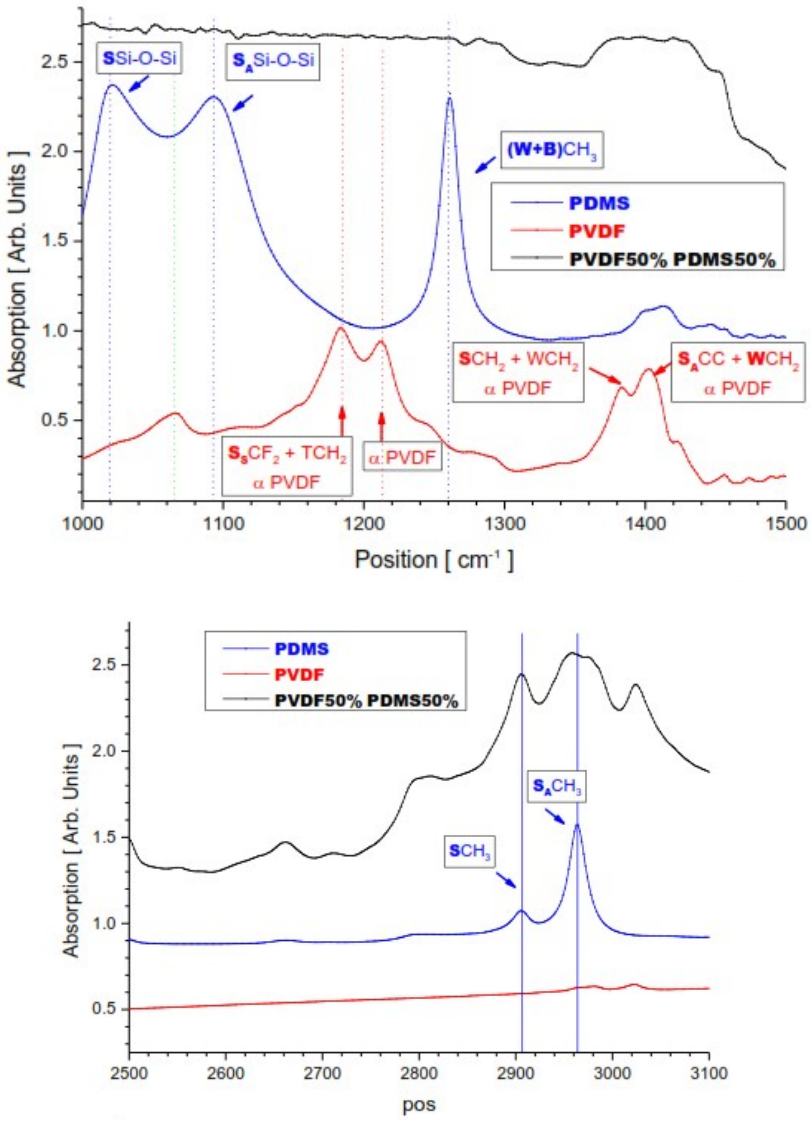

Fig. S3-4. FTIR Data: The figure shows the FTIR data for the blend and its constituents. FTIR shows the whole region in S3 and then splits up into various domains to further analyze the peaks. A clear analysis follows in the latter part of this section.

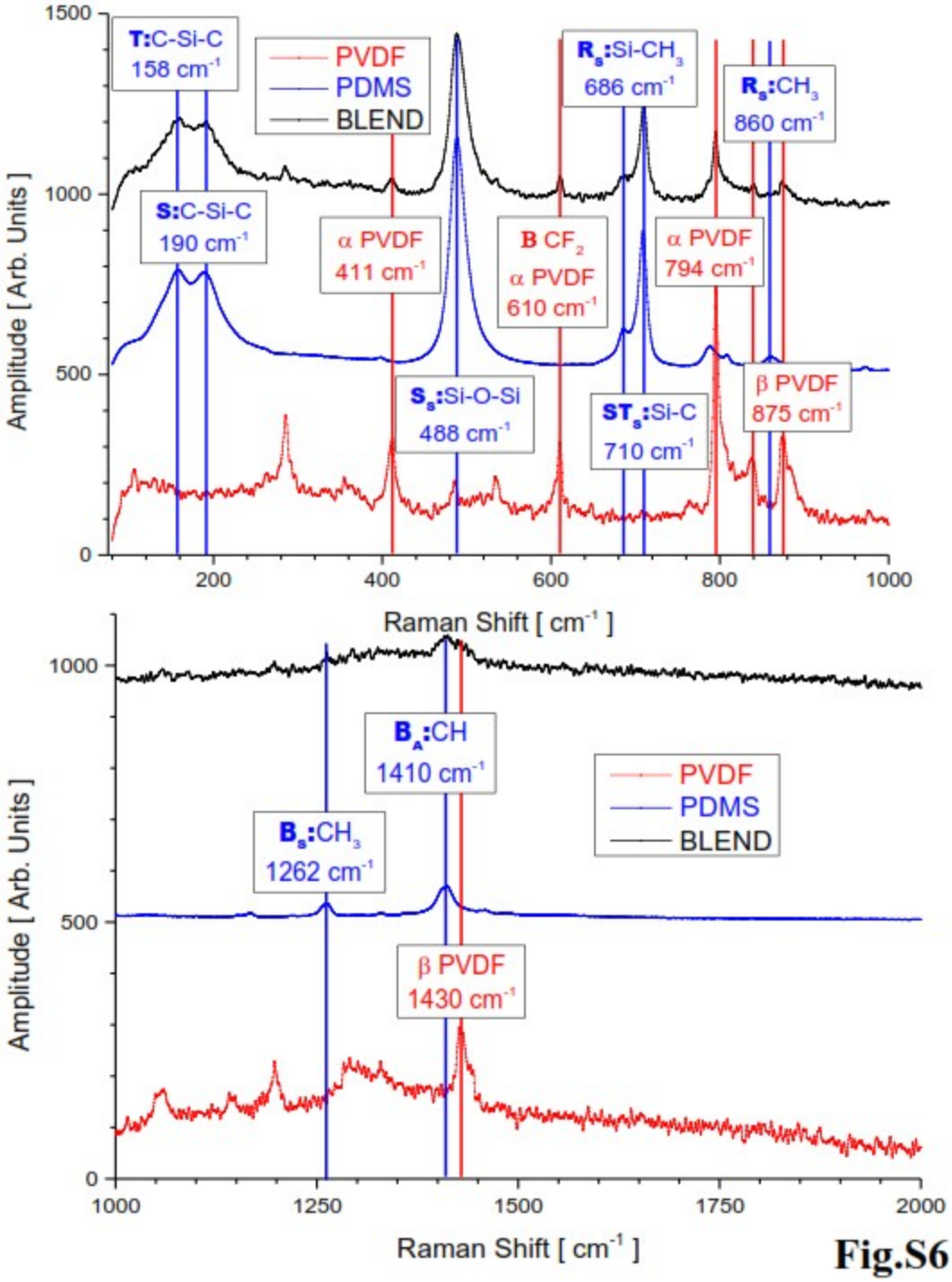
T:C-Si-C
158 cm-1
PVDF
PDMS
BLEND
Rs:Si-CH3
686 cm-1
Rs:CH3
860 cm-1
S:C-Si-C
190 cm-1
α PVDF
411 cm-1
B CF2
α PVDF
610 cm-1
α PVDF
794 cm-1
β PVDF
875 cm-1
Ss:Si-O-Si
488 cm-1
STs:Si-C
710 cm-1
Amplitude [Arb. Units]
Raman Shift [cm-1]
BA:CH
1410 cm-1
Bs:CH3
1262 cm-1
PVDF
PDMS
BLEND
β PVDF
1430 cm-1
Amplitude [Arb. Units]
Raman Shift [cm-1]

Fig.S6

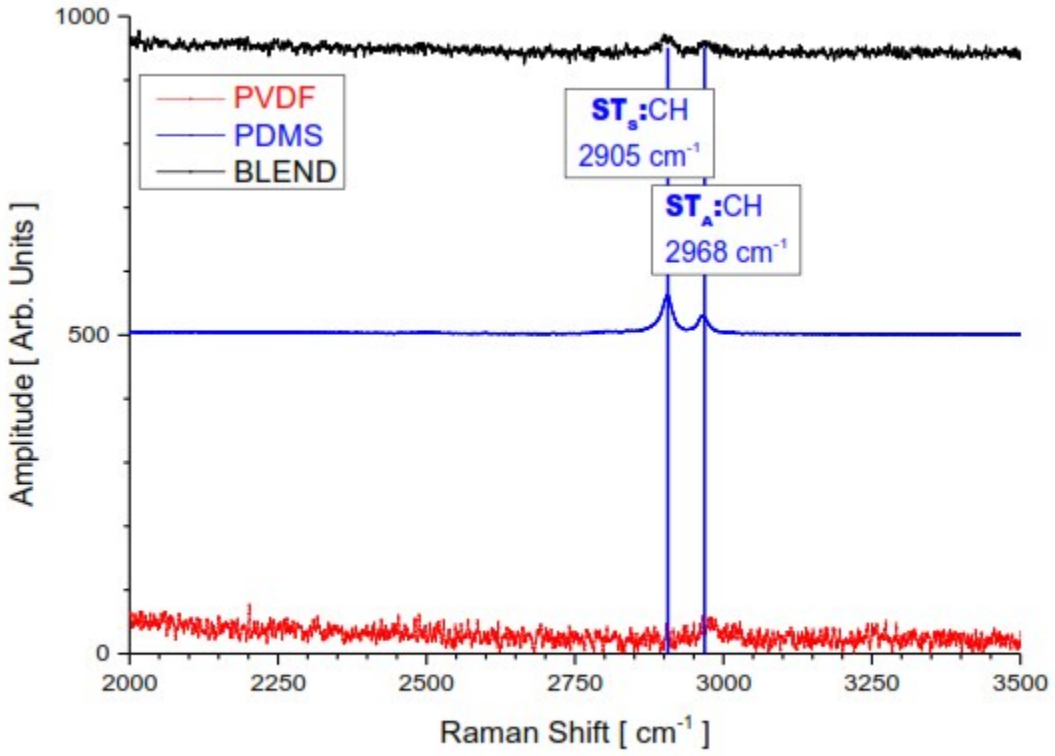

Fig. S5-7. Raman Data*:* The figure shows the Raman data for the blend and homopolymers. Raman shows no clear shifts and shows the presence of both homopolymers in the blend. Important peaks have been labeled in the graph. A concise discussion of the spectra follows in the next section.

Raman measurements were carried out using a Bruker Senterra confocal Raman microscope operating at 785 nm. The Raman spectrum, as seen in Fig. S6-7, of the blend, showed a clear convolution of the Raman spectra of the two homopolymers. The most intense peaks were noticed at 411 cm^{-1} and 610 cm^{-1} (assigned to CF_2 rocking and wagging/bending in PVDF, respectively) and at 487 cm^{-1} and 709 cm^{-1} (assigned to Si-O-Si symmetrical stretch and Si-C symmetrical stretch in PDMS, respectively). In the range 2750 cm^{-1} to 3200 cm^{-1}, it revealed a medium intensity peak at 2906 cm^{-1} and a weak intensity peak at 2964 cm^{-1} assigned

to CH_3 stretching in PDMS. A peak located at 2981 cm^{-1} and assigned to CH_2 vibrations in PVDF is also quite noticeable. The Raman revealed the presence of only alpha phase PVDF, and no peaks related to the beta or gamma phases. Overall, the spectra revealed that the general structure and bonding of the polymers in the blend was not altered.

Fourier Transform Infrared (FTIR) spectroscopy shows stark changes in the vibrational properties of the blend in relation to the homopolymers. The FTIR spectrum of the PVDF-PDMS blend, as seen in Fig. S3-5, in the range 425 to 725 cm^{-1} is consistent with an overlap of the lines noticed in PDMS and PVDF. However, the analysis is extended solely to the positions of the peaks, as the different amounts of PVDF, PDMS, and PVDF-PDMS samples do not allow a detailed analysis of the amplitude of the FTIR lines. In this range of wavelengths, no interactions between the two homopolymers were noticed. The most intense peak of the FTIR spectrum of the raw PDMS is located at 800 cm^{-1}. Significant changes can be seen ranging from 750 cm^{-1} to 1350 cm^{-1}. The strong decrease or even the disappearance of the PDMS peaks located at 800 cm^{-1} (assigned to rocking $Si(CH_3)_2$ groups and stretching Si-C-Si units), 865 cm^{-1} (assigned to the asymmetric rocking of CH_3 groups in $Si-CH_3$), 1020 cm^{-1} (assigned to the asymmetrical stretching of Si-O-Si bonds), at 1094 cm^{-1} (assigned to symmetrical stretching of Si-O-Si bonds), and at 1261 cm^{-1} (assigned to wagging and` bending motions of CH_3 groups) suggests an almost complete immobilization of large scale motions for the CH_3 groups of PDMS and a serious dampening of the Si-O-Si stretching modes. These motions are significantly affected in the blend, suggesting strong interactions between the PDMS and the F atoms of PVDF (via dipole-dipole or dipole-dipole induced interaction). Similar decreases of line amplitudes upon mixing

have been noticed for the PVDF homopolymer as the lines located at 762 cm^{-1} (bending of CF_2 in α PVDF), 794 cm^{-1} (bending of CH_2 in α PVDF), 975 cm^{-1} (CH out-of-the plane motions in α PVDF), 1184 cm^{-1} (symmetrical stretching of CF_2 and CH_2 in α PVDF), and 1212 cm^{-1} (assigned to α PVDF) have been drastically affected (decreased). A new, broad and complex spectrum is noticed in the blend, in the range 3500 to 4000 cm^{-1}. This range is typically assigned to single bond stretch and may be assigned to O-H bonds or to hydrogen bonds. The peak at 1408 cm^{-1}, assigned to asymmetric CH_3 bending in PDMS is wide and weak in the pristine polymer and may be also present in the final blend. The peak at 2964 cm^{-1} assigned to an asymmetric CH_3 stretch is observed both in PDMS and the blend[12]. These results indicate strong changes in the vibrations of the molecules and strong interactions beyond the purely mechanical interactions from the mixing.

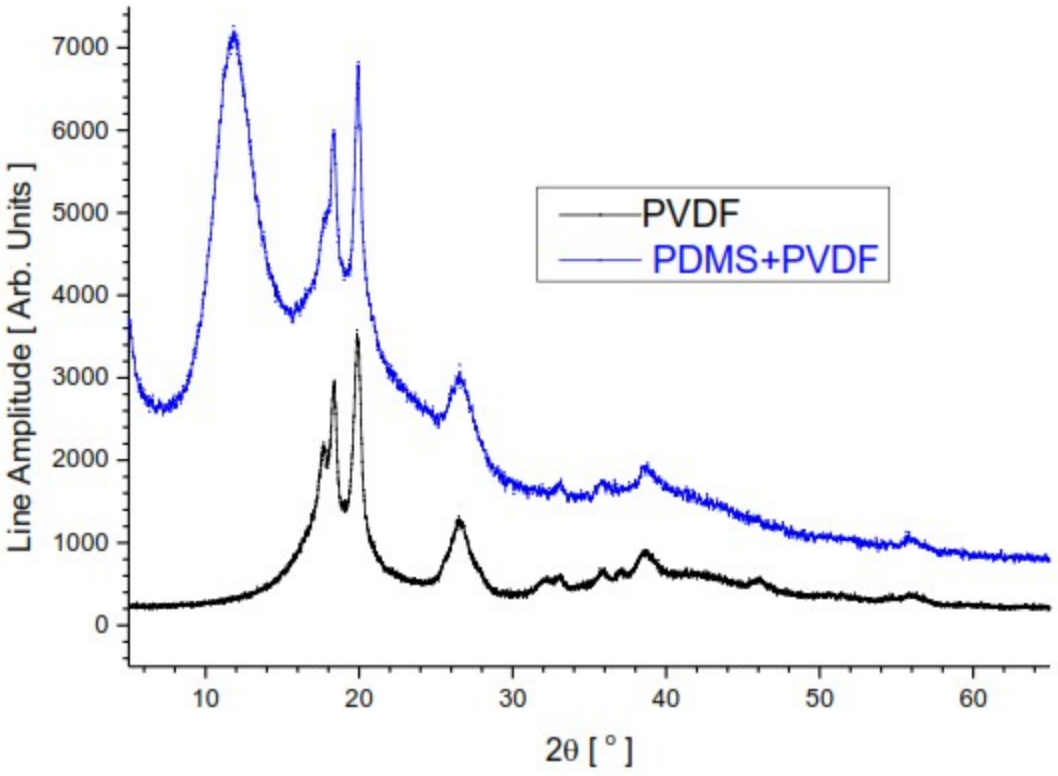

Fig. S8. XRD Data*:* The figure shows the XRD spectra for PVDF and the obtained blend. The data above indicates the presence of both materials in the blend. The wide peak at 12 degrees correlates to liquid PDMS and the others to the presence of alpha phase PVDF. This data backs up the Raman data previously shown.

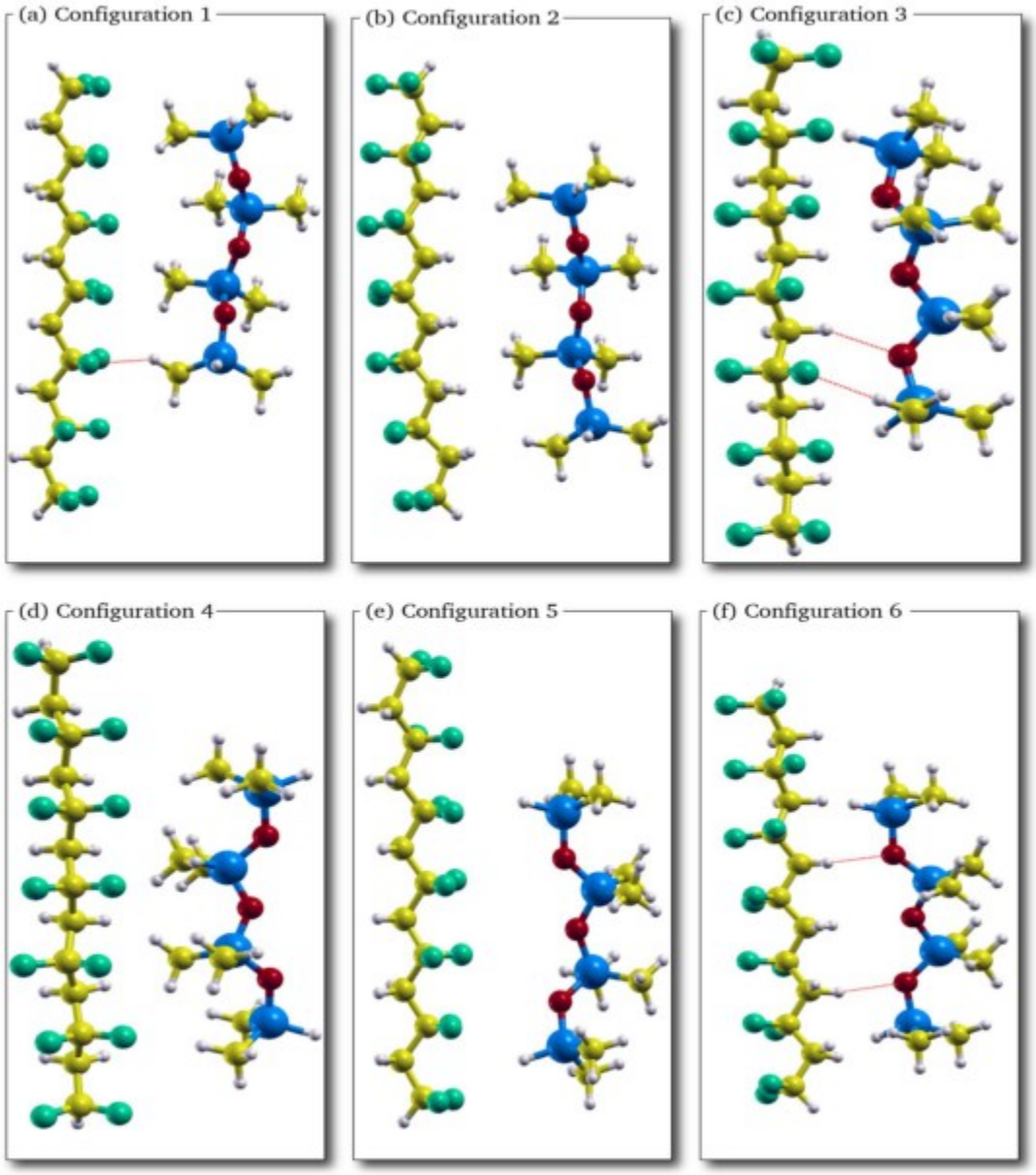

Fig. S9. Theoretical Modeling: The figure shows the assumed orientation of the polymers and their possible molecular interactions (marked as red lines).

The energies were obtained after a full optimization of the system geometry. The interaction between the polymers was computed using six different relative orientations

between the chains. Looking at the chains it is possible to identify two main regions. Taking the chain length as reference (x-direction, as shown in Fig. 2 a and b) the upper region is formed mostly by hydrogen, while the bottom one is formed by oxygens, in the case of PDMS, and fluorines for PVDF. Due to the electronegativity difference between the elements belonging to these two regions, both chains exhibit a dipole moment in the y-direction. For isolated chains, PDMS presents a dipole moment of 3.5 and PVDF 13.2 Debye. For orientations 1, 2, 4 and 5 (Fig. S9), the interaction energies are between 0.3 and 0.4 eV (Figure 2-f). Whereas, orientations 3 and 6 (Fig. 2 c and d, respectively) yield the two most stable configurations, with interaction energies of 0.7 and 1.1 eV, respectively.

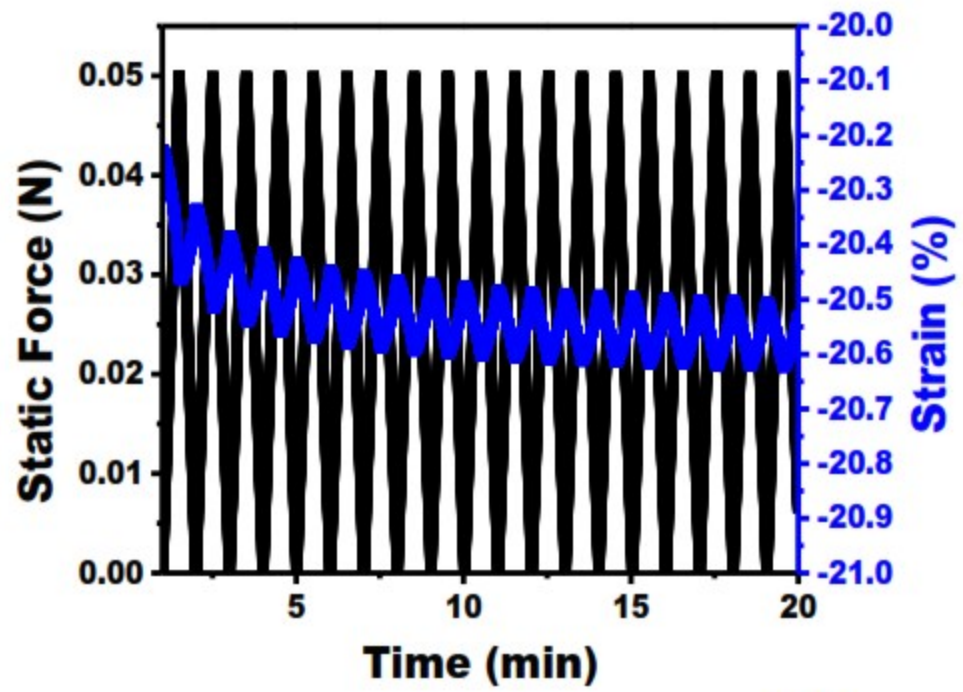
Static Force (N)
0.05
0.04
0.03
0.02
0.01
0.00
5
10
15
20
Time (min)
-20.0
-20.1
-20.2
-20.3
-20.4
-20.5
-20.6
-20.7
-20.8
-20.9
-21.0
Strain (%)

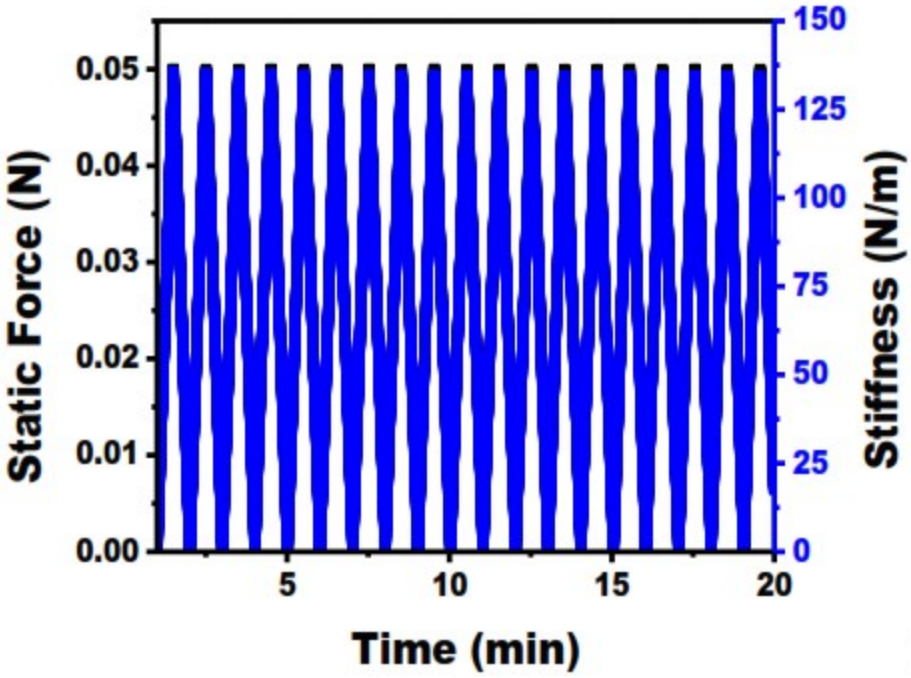
Static Force (N)
0.05
0.04
0.03
0.02
0.01
0.00
5
10
15
20
Time (min)
150
125
100
75
50
25
0
Stiffness (N/m)

Fig.S10

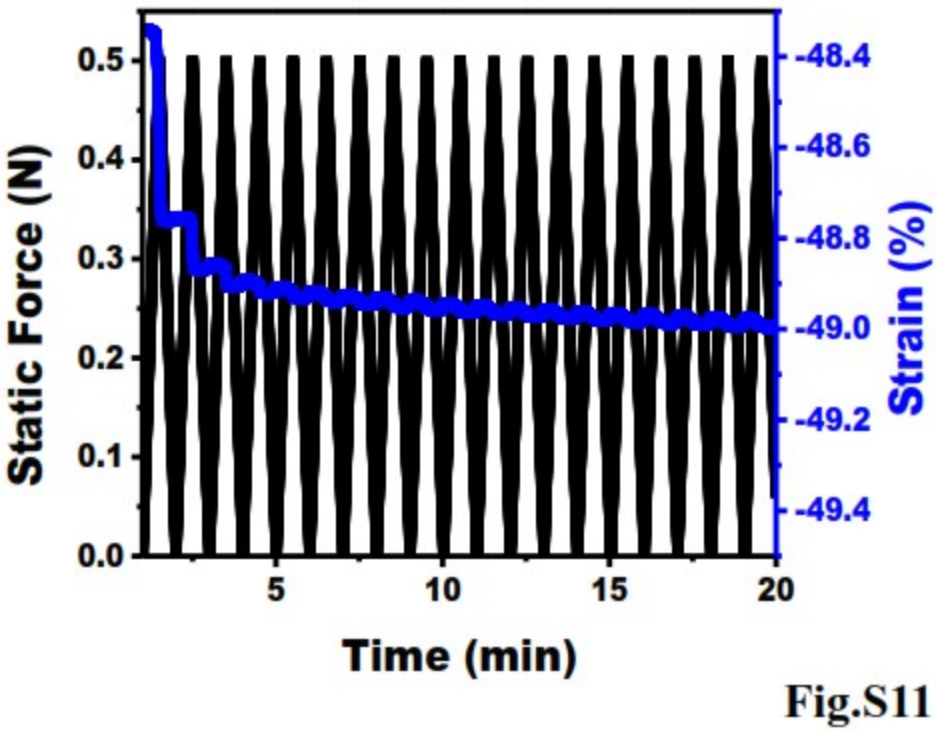

Fig. S10-11. DMA Load-Unload*:* The figures show loading at different values of the force. The data shows the gel behaves consistently in all tests. Additionally, no clear loss of stiffness is observed as the tests ran.

A measurement of the stiffness shows that during the first cycle it follows the same trend as the loading and in the second cycle presents a different behavior (Fig. S10 - supplementary material). During initial loading the stiffness increases as the applied load increases but reaches a maximum value (around 7500 N/m) before the end of the compression procedure (Fig. S10 - supplementary material). After achieving the maximal load, the stiffness exhibits smooth decreasing behavior even whilst loading is still underway. The maximum stiffness (around 8100 N/m) is achieved during the third cycle. During the completed load-unload (compression-decompression) procedure the sample showed a permanent deformation of 1%,

9%, and 6% in each cycle, respectively. The stiffness behavior presented during the second cycle indicates the presence of two regimes during the compression step. Details about the mechanism behind such behaviors are explained in the latter part of the paper. The loss of strain during compression (loading) and decompression (unloading) is most likely due to the re-arrangement of the PVDF spheres in the liquid phase. The low irreversibility of the third cycle as compared to the second cycle is due to the increased strain rate. Due to an increased strain rate, there is not enough time for the spheres to re-orient.

Whilst undergoing cycling, the blend showed a slight loss of stiffness (> 1%) until an equilibrium point was reached, which would be expected if the PVDF spheres were re-organizing into a lower energy state. This hypothesis is also supported by testing at higher loads (Fig. S10 - supplementary material). During unloading or separation, the interaction between the spheres and the liquid accommodates the strain and gives rise to resistance to cohesion which gives rise to the strain lines seen in SEM. The adhesive properties on different substrates come from the system morphology enhanced by the PVDF spheres dispersed in the PDMS medium, creating a solid-liquid system, which can interact by the electrostatic dipole. In addition, due to the large contact surface area of the PVDF spheres, they prevent flow acting as anchors in the blend. The surface area acts synergistically with the dipoles thus creating a very strong intermolecular interaction. The blend emulates tree frogs and when in contact with any surface maximizes the surface area by wetting and removing all gases thus creating strong adhesion between different substrates.

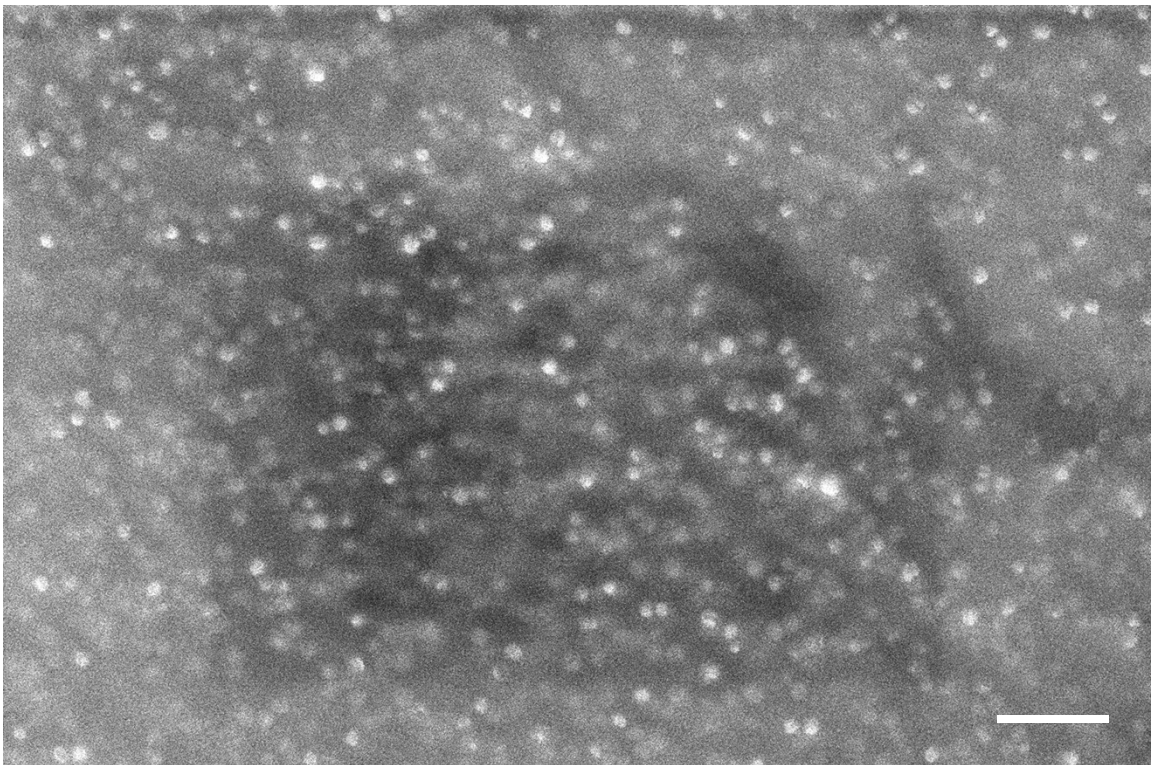

Fig. S12. SEM of PDMS (matrix), PVDF (particles of bright contrast), scalebar is 1micro-meter.

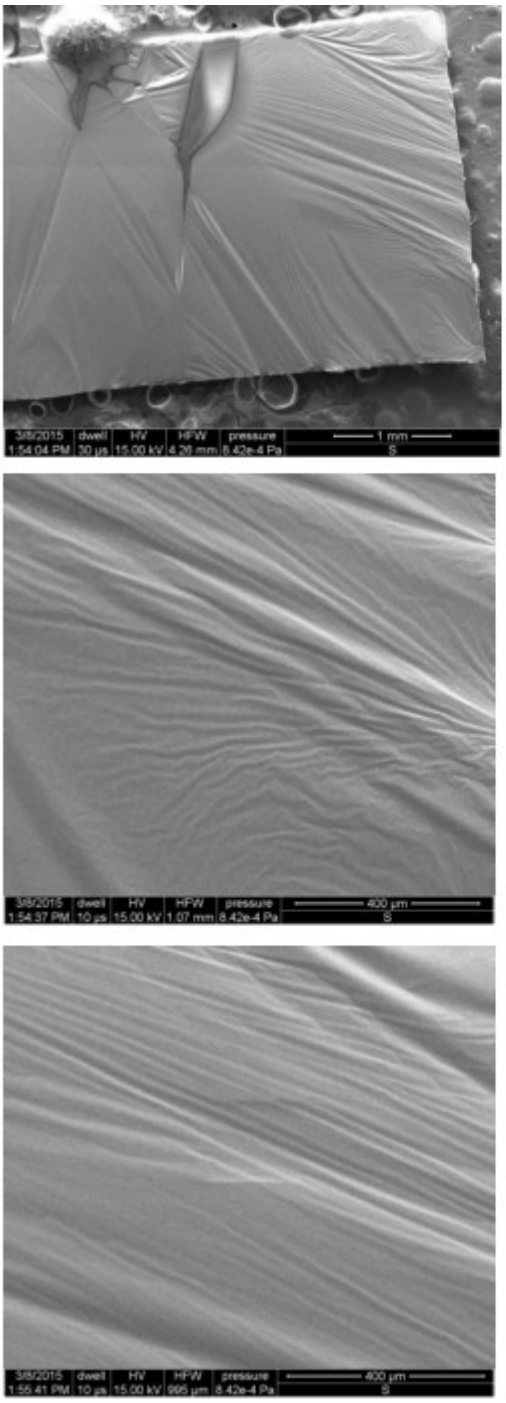

Fig. S13. SEM of PDMS: The figure shows the SEM of PDMS. This shows the stress lines created by the gold coating on the PDMS post sputtering.

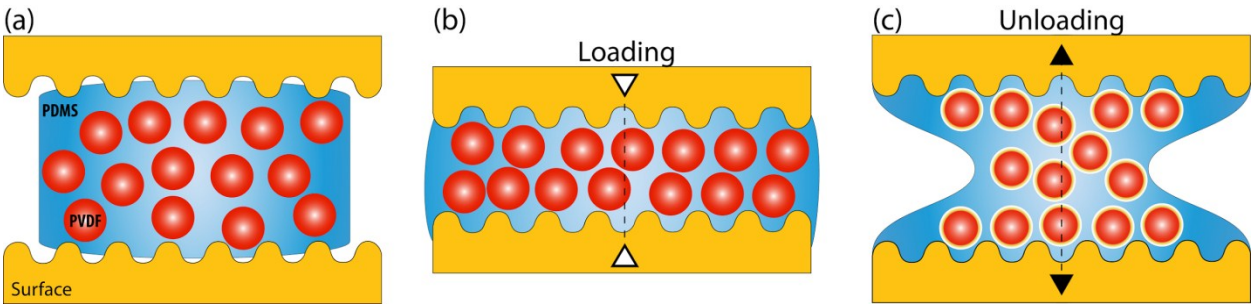

Fig. S14. Schematic representation of the loading/unloading steps: The figure shows schematically the system arrangement during the loading step. (a) the PVDF spheres (red) are dispersed in the PDMS (blue) medium. (b) The loading step induces a rearrangement in the PVDF spheres, increasing the number of spheres in contact with the substrate (in yellow). (c) During the unloading step, the PVDF spheres strongly interact with the substrate and with the PDMS, creating the adhesive behavior.